Journal of Applied Polymer Science

Toward Environment-Friendly Composites of Poly(ε-caprolactone) Reinforced with Stereocomplex-Type Poly(L-lactide)/Poly(D-lactide)

Yi Li,[1,2] Qinglin Dong,[1] Changyu Han,[1] Yijie Bian,[1] Xin Zhang,[1] Lisong Dong[1]

[1]Key Laboratory of Polymer Ecomaterials, Changchun Institute of Applied Chemistry, Chinese Academy of Sciences, Changchun 130022, China

[2]College of Material Science and Engineering, Jilin Jianzhu University, Changchun 130118, China

Correspondence to: C. Han (E-mail: cyhan@ciac.ac.cn)

ABSTRACT: In this work, stereocomplex-poly(L- and D-lactide) (sc-PLA) was incorporated into poly(ε-caprolactone) (PCL) to fabricate a novel biodegradable polymer composite. PCL/sc-PLA composites were prepared by solution casting at sc-PLA loadings of 5–30 wt %. Differential scanning calorimetry (DSC) and wide-angle X-ray diffraction (WAXD) demonstrated the formation of the stereocomplex in the blends. DSC and WAXD curves also indicated that the addition of sc-PLA did not alter the crystal structure of PCL. Rheology and mechanical properties of neat PCL and the PCL/sc-PLA composites were investigated in detail. Rheological measurements indicated that the composites exhibited evident solid-like response in the low frequency region as the sc-PLA loadings reached up to 20 wt %. Moreover, the long-range motion of PCL chains was highly restrained. Dynamic mechanical analysis showed that the storage modulus (E') of PCL in the composites was improved and the glass transition temperature values were hardly changed after the addition of sc-PLA. Tensile tests showed that the Young's modulus, and yield strength of the composites were enhanced by the addition of sc-PLA while the tensile strength and elongation at break were reduced. © 2013 Wiley Periodicals, Inc. J. Appl. Polym. Sci. **2014**, *131*, 40208.

KEYWORDS: poly(ε-caprolactone); blends; mechanical properties

Received 26 September 2013; accepted 18 November 2013

DOI: 10.1002/app.40208

INTRODUCTION

Biodegradable poly(ε-caprolactone) (PCL) is one of the most important environment-friendly materials for its excellent performance such as biodegradable, biocompatible, and thermoplastic properties. The copolymers of PCL and itself have already achieved commercial success. Nevertheless, the low melting point and modulus, poor stability, and easy to deformation of PCL have restrict its application.[1–6] Therefore, many attentions have been paid on the PCL based polymer blends in order to solve aforementioned shortcomings.[6–16] For instance, Wischke et al. investigated the PCL/poly[(e-caprolactone)-*co*-glycolide] blends in which the advantageous properties of both components could selectively be combined.[6] Xing et al. investigated crystallization, melting behavior, and wettability of PCL and PCL/poly(N-vinylpyrrolidone) (PVP) blends. They found that PVP had a restrain effect on the crystallization of PCL and the hydrophilic properties of PCL/PVP blends were improved compared with pure PCL.[7] Moreover, compounding PCL with layer silicate,[16–18] carbon nanotubes,[1,15,19] or fumed silica[8,9,20,21] has been widely investigated. For example, in previous research, PCL/silica nanocomposites were prepared by melt compounding. It was found that the presence of silica could provide a number of heterogeneous nucleation sites for the PCL crystallization while the aggregates of silica could restrict crystal growth of PCL. However, the crystal structure of PCL remained almost unchanged after nanocomposites preparation.[8]

Poly(lactic acid) (PLA) has been paid considerable attention from both fundamental and practical perspectives because it is derived completely from renewable resources, and hence production is sustainable, but also it can significantly contribute to the control of green-house gas (CO_2) emission as a result of carbon capture during plant growth and the eventual complete biodegradability of the PLA matrix.[22–27] PLA has two stereoregular enantiomers, poly(L-lactide) (PLLA), and poly(D-lactide) (PDLA) due to the presence of a chiral carbon in the skeletal chain. A special crystalline structure termed stereocomplex based on $CH_3\ldots C{=}O$ interactions of stereoselective van der Waals forces can be formed by blending PLLA and PDLA. This stereocomplex-PLA (sc-PLA) showed its T_m at about 230°C, which was about 50°C higher than that of pure PLLA or PDLA, so that sc-PLA should accordingly have better thermal and mechanical properties, and higher hydrolytic stability than neat PLLA or PDLA.[28–30]

Although the properties of PCL/PLA blends have been extensively studied,[31–34] however, to the best of our knowledge,

environment-friendly composites of PCL reinforced with sc-PLA have not been explored in details. Therefore, in this work, a series of PCL/sc-PLA composites are prepared by solution blending. The effects of the sc-PLA on the crystallization, rheological behavior, and mechanical properties of the PCL were investigated. However, the sc-PLA has higher strength, modulus, making it an ideal biomaterial for load bearing devices. In contrast, PCL shows weaker modulus and yield strength, making it a preferred candidate for developing the low strength scaffolding material. Consequently, blending sc-PLA and PCL can balance the mechanical properties and obtain the composites with the controllable and improved performances, which might be of great interest for its wide practical application as packing materials and biomaterials.

EXPERIMENTAL

Materials and Sample Preparation

PCL (MFI 5 g/10 min) was a commercial product, CAPA6800 (Solvay Interox). PLLA (4032D) was a commercial product of NatureWorks. It exhibited a weight-average molecular weight (M_w) of 207,000, polydispersity of 1.73. D-isomer content of PLLA is ~2.0%. PDLA were synthesized by the ring-opening polymerization of D-lactide using tin octanoate as a catalyst. It exhibited a M_w of 110,000, polydispersity of 1.92.

Ternary blends comprising PCL, PLLA, and PDLA were first separately prepared, then stereocomplexing sc-PLA and PCL mixtures were prepared using solvent-mixing, followed with film-casting. PCL was first dissolved in chloroform ($CHCl_3$) solution, and then further blended with solutions of PLLA and PDLA with proper ratios. Ratios of PLLA to PDLA in blends were maintained at 1/1 by weight in ternary blends. In ternary blends, PLLA/PDLA was fixed at 1/1, with the PCL contents ranging from 95/5 to 70/30 in weight ratios, the first number referring to the weight percentage of PCL. The prepared solutions were mixed together with vigorous stirring, the solutions were cast onto petri dishes placed horizontally, and then the solvent was allowed to evaporate at room temperature for 12 h. The sample was further dried at 40°C under vacuum for 7 days to remove the solvent completely. For convenience, neat PCL and its composites were, respectively, designated as neat PCL and PCLX in the following discussion, where X representing the sc-PLA content (wt %) of the composite.

Characterizations and Measurements

The morphology of the fractured surface, which was prepared under liquid nitrogen was observed using a field emission scanning electron microscopy (ESEM; FEI, Eindhoven, The Netherlands) at an accelerating voltage of 12 kV. The fracture surface was coated with a thin layer of gold before the measurement.

Thermal analysis was performed using a TA Instruments differential scanning calorimetry (DSC) Q20 with a Universal Analysis 2000. Samples weights were in the range of 5–8 mg. The effects of the sc-PLA on the crystallization behavior of the PCL were investigated. All specimens were heated from 40 to 100°C at a heating rate of 100°C/min to erase any thermal history. Then they were cooled to −20°C at a cooling rate of 10°C/min (first cooling). The specimens were further heated to 250°C again from −20°C at a heating rate of 10°C/min to study the subsequent melting behavior (second heating). The degree of crystallinity of the PCL was calculated by the following equations[35]:

$$x_{c,\mathrm{PCL}}(\%) = (\Delta H_t - \Delta H_{g,\text{sc-PLA}} \cdot X_{\text{sc-PLA}})100/[(1 - X_{\text{sc-PLA}})142] \quad (1)$$

$$X_{sc-PLA} = W_{\text{sc-PLA}}/(W_{PCL} + W_{\text{sc-PLA}}) \quad (2)$$

where $W_{\text{sc-PLA}}$ and W_{PCL} were the weights of sc-PLA and PCL, respectively, in the composites. ΔH_t (J/g of polymer) was the enthalpy of overall transition including the glass transition enthalpy of sc-PLA and melting enthalpy of PCL. Here, we assumed the $\Delta H_{g,\ \text{sc-PLA}}$ as zero because it was tiny to neglected, and 142 (J/g of PCL) was the melting enthalpy of PCL with 100% crystallinity reported by Crescenzi et al.[36] To investigate the effect of degree of crystallinity of PCL on the static mechanical properties of the composites, the degree of crystallinity values of all the samples prepared via the compression-molded process were also obtained from the first heating traces at a rate of 10°C/min.

Wide angle X-ray diffraction (WAXD) experiments were performed on a D8 advance X-ray diffractometer (Bruker, Germany) at room temperature in the range of 5–40° with a scanning rate of 3°/min. The Cu K_α radiation ($\lambda = 0.15418$ nm) source was operated at 40 kV and 200 mA. The samples were first hot-pressed into films with a thickness of around 1.0 mm at 120°C.

Rheological measurements were carried out on a rheometer (AR2000EX, TA Instruments-Waters LLC) equipped with a parallel plate geometry using 20-mm diameter plates. The sheet samples in thickness of 1.0 mm were molten at 100°C in the fixture and experienced dynamic frequency sweep. The oscillatory frequency swept ranging from 100 to 0.01, with a fixed strain of 1%.

Dynamic mechanical analysis (DMA) was performed on the samples of 20.0 × 4.0 × 1.0 mm^3 in size using a dynamic mechanical analyzer from Rheometric Scientific under tension mode in a temperature range of −80 to 0°C at a frequency of 1 Hz and 3°C/min.

The static mechanical properties of neat PCL and various composites were determined by using an Instron 1211 testing machine. The test was carried out with crosshead speed of 100 mm/min at room temperature in the tensile mode. The values reported were averages for at least five dumbbell-shaped specimens with necks of 20.0 mm long and cross-sectional areas of 4.0 × 1.0 mm^2.

RESULTS AND DISCUSSION

Morphology of Neat PCL and Its Composites

It is well known that the dispersion of another additive in the polymer matrix will greatly influences the physical properties of polymer matrix. To investigate the dispersion of sc-PLA in the PCL matrix, the fracture surfaces of neat PCL and its composites were observed by ESEM. The morphology of the samples was shown in Figure 1. Figure 1(a) shows ESEM micrograph of the neat PCL fracture surface for comparison, which was smooth and featureless. Figure 1(b–e) shows ESEM micrographs of the PCL5

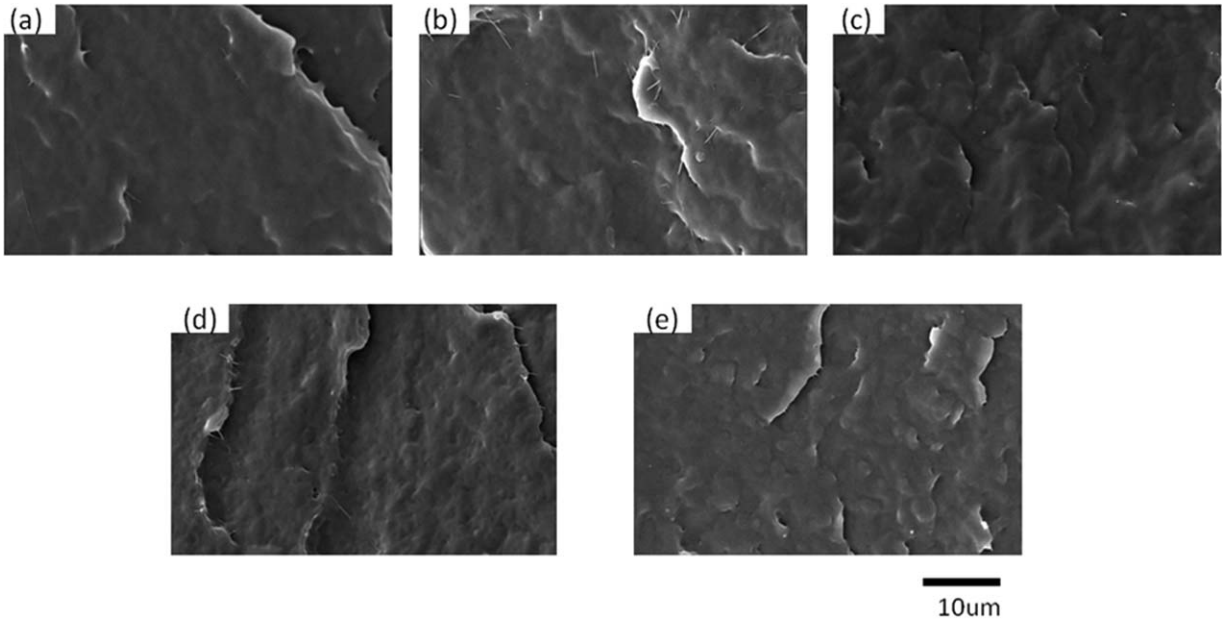

Figure 1. ESEM microphotographs of the fractured surfaces of (a) neat PCL, (b) PCL5, (c) PCL10, (d) PCL20, and (e) PCL30.

to PCL30 fracture surface, respectively. However, as unexpected, the fracture surfaces of the PCL composites with various sc-PLA loadings were also smooth and featureless. A typical phase-separated morphology with sc-PLA dispersed in PCL matrix was not observed. It was believed that the result was due to the good compatibility between PCL and sc-PLA, which was also contributed to the improved mechanical properties and rheological properties of the composites as discussed below.

Nonisothermal Crystallization and Melting Behavior

The nonisothermal melt crystallization and subsequent melting behavior of neat PCL and various composites were studied by DSC. Figure 2 shows the DSC thermograms of the first cooling traces and second heating traces, respectively, for neat PCL and its composites with different compositions. All parameters derived from the DSC curves were summarized in Table I. In Figure 2(a), the crystallization onset temperature (T_c^{onset}) and crystallization peak temperature (T_c) were both increased with increasing the content of sc-PLA. The T_c^{onset} and T_c of neat PCL were 32.9 and 24.8°C, respectively. With the addition of 5 wt % of sc-PLA, the T_c^{onset}, and T_c of PCL increased to 33.3 and 25.6°C, respectively, and the crystallization proceeded within a narrower temperature range. With the sc-PLA content increased to 10 wt %, the T_c^{onset} and T_c of PCL in the composites decreased to 33.2 and 25.5°C, respectively, but still higher than those of neat PCL. Further increasing sc-PLA, the T_c^{onset} unchanged while the T_c kept increasing. The increase of crystallization temperature, induced by the addition of sc-PLA, indicated that sc-PLA acted as the heterogeneous nucleating agent by lowering the free energy barrier toward nucleation and thus enhanced the crystallization of PCL in the composites. However, the crystallization enthalpy (ΔH_c) of PCL in the composites varied slightly with increasing the sc-PLA content, indicating that the addition of sc-PLA showed little effect on the final crystallinity of the PCL in the composites.

Figure 2(b) shows the subsequent melting traces of neat PCL and its composites after cooling from the melt at 10°C/min (second heating). Neat PCL exhibited a melting temperature (T_m) of 57.3°C with melting enthalpy (ΔH_m) being 54.1 J/g. Meanwhile, the composites with various sc-PLA contents showed a T_m of 55–57°C. It was clear that the addition of sc-PLA showed little effect on the variation of T_m, indicating that the lamellar thickness of the PCL crystal was unchanged. The χ_c of PCL listed in Table I increased slightly from 38.1 to 40.2% with increasing the sc-PLA content to 10 wt %. However, the value of χ_c decreased slightly with further increasing of sc-PLA. Moreover, formation of the stereocomplex in the blends was also confirmed by the subsequent melting traces of PCL composites after cooling from the melt. In all the samples, the stereocomplex melting peak was present around 224.2°C as reported in the literature [23]. The area of the melting endotherm for the stereocomplex increased as the amount of PLLA and PDLA in the blend increased showing that the initial composition of the blend could be used to control the amount of stereocomplex in the final material.

Effect of sc-PLA on the Crystal Structure of PCL

WAXD experiments were performed to investigate the effect of the addition of sc-PLA on the crystal structure of PCL. Figure 3 shows the WAXD patterns of neat PCL and its composites. Neat PCL presented main diffraction peaks at 21.3 and 23.6, corresponding to 110 and 200 planes, respectively.[37,38] The composites also exhibited nearly the same diffraction peaks at the same locations, indicating that the addition of sc-PLA did not alter the crystal structure of PCL. Moreover, the most intense peaks of the sc-PLA samples were observed at 2θ values of 12, 21, and 24°. These peaks are for the stereocomplex crystallized

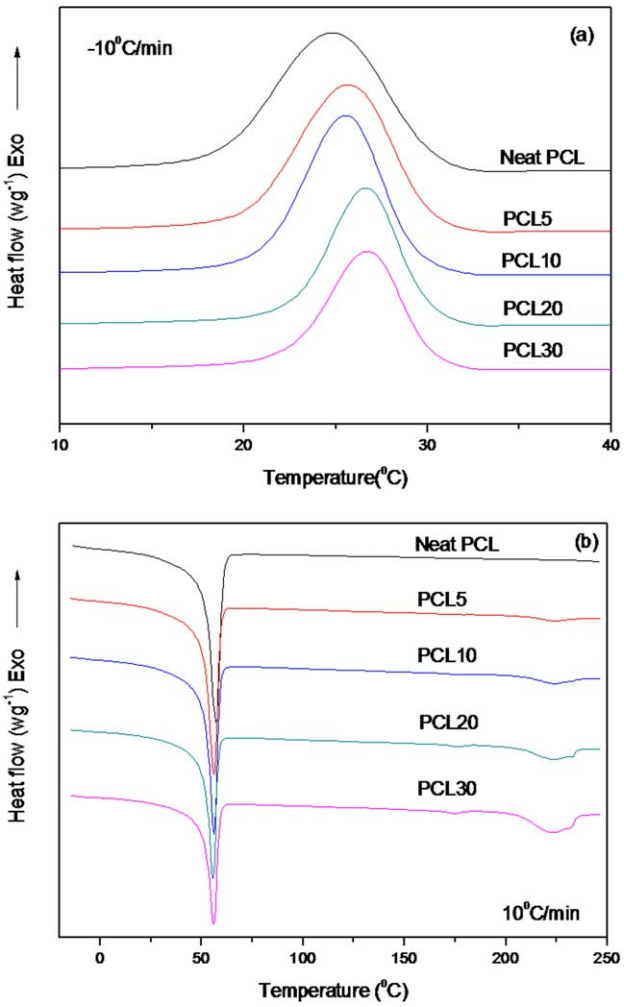

Figure 2. DSC curves of (a) nonisothermal melt crystallization and (b) subsequent melting for various formulations. [Color figure can be viewed in the online issue, which is available at wileyonlinelibrary.com.]

in a triclinic unit cell of dimensions: $a = 0.916$ nm, $b = 0.916$ nm, $c = 0.870$ nm, $\alpha = 109.2°$, $\beta = 109.2°$, and $\gamma = 109.8°$, in which L-lactide and D-lactide segments were packed parallel taking 3_1 helical conformation.[28,30] However, only a peak of the blended samples at 2θ values of 12° could be observed due to the formation of the stereocomplex in the blends. Two peaks at

Table I. Thermal and Crystalline Properties of PCL in the Composites

Samples	T_c^{onset} (°C)	T_c (°C)	ΔH_c[a] (J/g)	T_m (°C)	ΔH_m[a] (J/g)	$\chi_{c,PCL}$ (%)
Neat PCL	32.9	24.8	54.6	57.3	54.1	38.1
PCL5	33.3	25.6	52.3	56.1	56.7	40.0
PCL10	33.2	25.5	53.4	56.2	57.1	40.2
PCL20	33.2	26.6	46.5	55.5	52.5	37.0
PCL30	33.2	26.8	48.2	56.0	53.7	37.8

[a] ΔH_c and ΔH_m are corrected for the content of PCL in the composites.

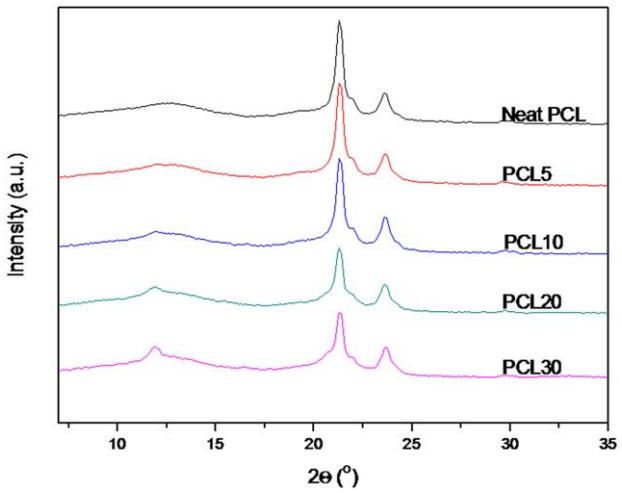

Figure 3. WAXD patterns of neat PCL and its composites. [Color figure can be viewed in the online issue, which is available at wileyonlinelibrary.com.]

2θ values of 21° and 24° were overlapped by the two corresponding peaks of PCL, respectively.

Rheological Behavior of Neat PCL and Its Composites

Since the viscoelastic properties are highly related to both the dispersion state of filler and the interactions between filler and polymer matrix, rheology is a powerful tool to investigate microscopic and mesoscopic structure of the filled polymer systems. The dependence of dynamic storage modulus (G') and complex viscosity (η^*) for the neat PCL and its composites at 100°C was showed in Figure 4(a,b), respectively. Similar with PCL/silica and PLA/silica systems reported previously,[8,20] the G' of PCL/sc-PLA composites also increased greatly with the addition of sc-PLA. It was seen that neat PCL sample shows typical terminal behavior at low frequencies with the scaling properties of $G' \propto \omega^2$, which was in consistent with the linear viscoelastic theory. Nevertheless, this terminal behavior disappeared gradually with an increase in sc-PLA loadings. As the sc-PLA loading reached up to 20 wt %, the sample exhibited evident solid-like response in the low frequency region, indicating occurrence of an elastic deformation dominated flow. At this loading level, the interactions among the sc-PLA phase were strong enough, and as a result leaded to the formation of percolated sc-PLA network structures. In this case, the large-scale relaxations of PCL chain coils were highly restrained by the presence of sc-PLA, and hence the PCL/sc-PLA composite showed a solid-like flow behavior at the low-frequency region. As a result, the low-frequency η^* increased with an increase in sc-PLA loadings, and the Newtonian plateau disappeared gradually as shown in Figure 4(b).

As soon as the composites percolated, the large scale polymer chain relaxation behaviors might be highly affected by the percolated sc-PLA network. Figure 5 shows the Han plots of $G' = G''$[39] for neat PCL and its composites at 100°C, respectively. In addition, the reduced slope with the addition of sc-PLA indicated that the composites became more heterogeneous. It should be noted that the inflection point where the slope was changed shifts to a higher frequency with an increase in sc-PLA loadings. This indicated that much energy was needed

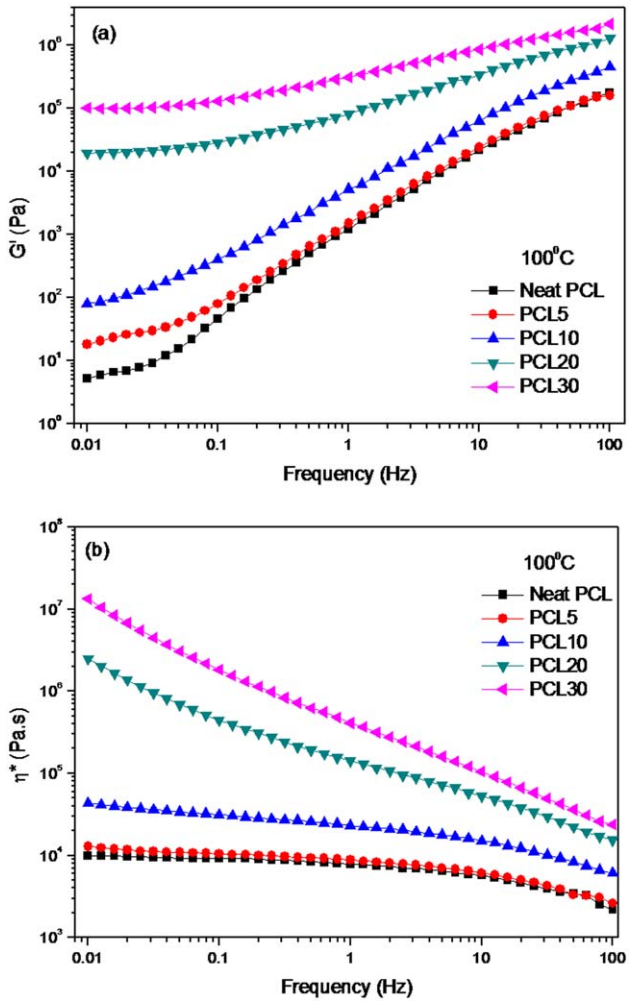

Figure 4. (a) Dynamic storage modulus (G') and (b) complex viscosity (η^*) for neat PCL and its composites at 100°C obtained in dynamic frequency sweep. [Color figure can be viewed in the online issue, which is available at wileyonlinelibrary.com.]

to change the degree of heterogeneity due to the increased physical association within the composites at a high sc-PLA loading. The physical association between sc-PLA and PCL matrix changed the relaxation behavior of the PCL chain inevitably.[40] The relaxation time (λ) could be calculated as follows:

$$\lambda = \frac{G'}{\eta^* \times \omega^2} \tag{3}$$

The calculated ratio of the relaxation time of composites to that of neat PCL ($\Delta\lambda$) increased gradually with sc-PLA loadings and, finally to about 2.7, 3.5, 14.9, and 14.4 for PCL5, PCL10, PCL20, and PCL30 samples at the low frequency (0.01 Hz) at 100°C, respectively. This indicated that the role of sc-PLA to make the PCL chain need longer time for the relaxation became stronger with an increase in sc-PLA loadings. The presence of sc-PLA greatly restricted the chain mobility of PCL matrix once percolation network structure forms.

This strong restriction was further confirmed by the Cole–Cole[41] plots shown in Figure 6. The single arc of the neat PCL

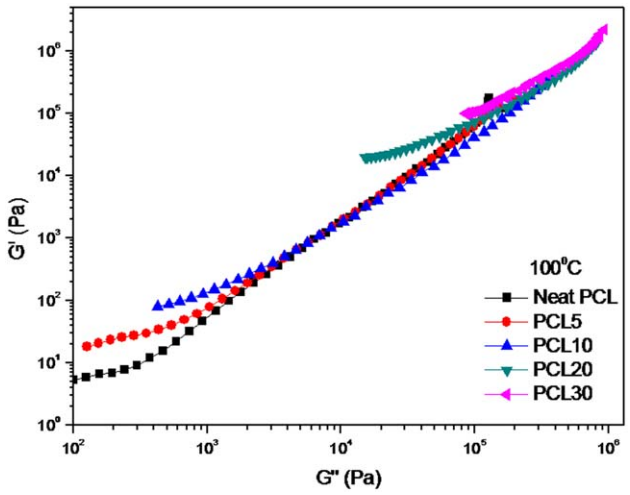

Figure 5. Han plots of dynamic storage modulus (G') versus dynamic loss modulus (G'') at 100°C for neat PCL and its composites. [Color figure can be viewed in the online issue, which is available at wileyonlinelibrary.com.]

represented relaxation process with a relaxation time distribution. For PCL5 and PCL10 samples, the Cole–Cole plots were divided into two parts: A half-baked arc at low viscosities corresponding to the local dynamic of PCL and, a rigid tail at high-viscosity region, which was indicative of the long-term relaxation of those restrained PCL chains, respectively. The upturn between these two parts presented remarkable shift to the high-viscosity region with an increase in sc-PLA loadings. As the loading up to 20 wt %, the local relaxation arc of PCL nearly disappeared, indicating that the long-term relaxation of those restrained PCL chains became the dominant one in the whole relaxation behaviors of the PCL composites. This also confirmed that the mesostructure of percolation network forms at present sc-PLA loading, and the long-range motion of PCL chains were highly restrained consequently. Very similar linear viscoelasticity behaviors of PLA/silica and PCL/silica nanocomposites were also observed in previous works.[9,20]

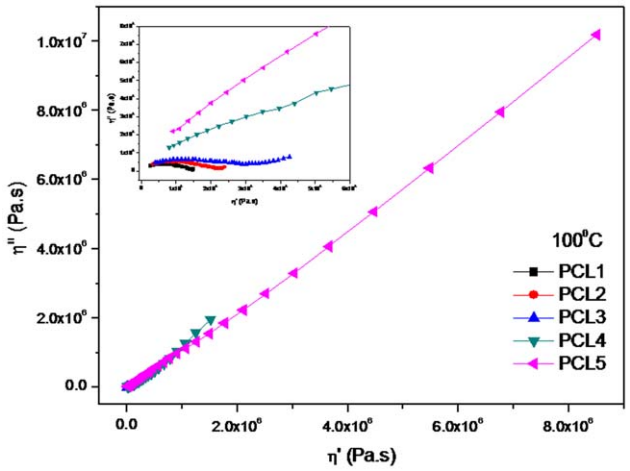

Figure 6. Cole–Cole plots of imaginary viscosity (η'') versus real viscosity (η') for neat PCL and its composites at 100°C. [Color figure can be viewed in the online issue, which is available at wileyonlinelibrary.com.]

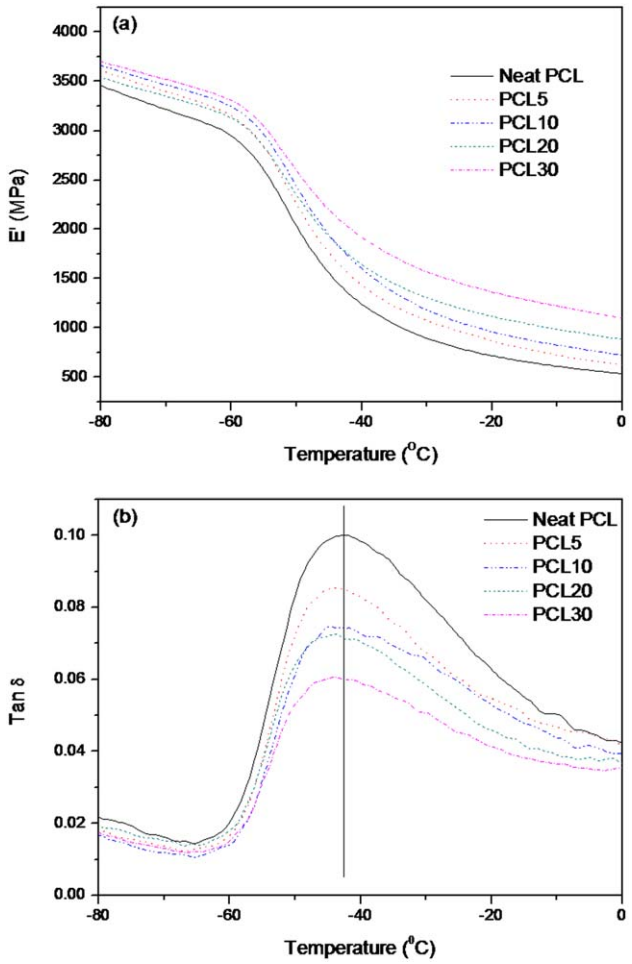

Figure 7. Temperature dependence of (a) storage modulus (E') and (b) tanδ for neat PCL and its composites. [Color figure can be viewed in the online issue, which is available at wileyonlinelibrary.com.]

Dynamic Mechanical Analysis

Results of DMA carried out over a range of temperatures at a constant frequency of 1 Hz were shown in Figure 7. It was clear from storage modulus (E') versus temperature curves [Figure 7(a)] that E' of the composites was higher than that of neat PCL throughout the temperature range from −80 to 0°C. Moreover, E' increased with increasing sc-PLA content at the same temperature, indicating that the sc-PLA had strong influence on the elastic properties of the PCL matrix. For all the samples, the E' decreased sharply in the range of −50 to −30°C due to the glass transition of PCL. Below the glass transition temperature (T_g), the enhancement of E' was slight in the PCL composites, while above T_g, the enhancement of E' was significant. The measured E' values at −75°C and 0°C were given in Table II. At −75°C, the E' was increased from 3331 MPa for neat PCL to 3607 MPa for the composite with 30% sc-PLA. Only an increase of 8% was obtained as compared with that of the neat PCL. While at 0°C, the E' was increased from 535 MPa for neat PCL to 1104 MPa for the composite with 30% sc-PLA. A significant increase in E' was 106% for the composites as compared to that of the neat PCL, indicating that the sc-PLA was an effective reinforcing agent for PCL. The increase in E' of PCL/sc-PLA composites could be attributed to the high stiffness of the sc-PLA, which introduced rigid interface into the composites. This provided better stress transfer ability and increase in E' of the PCL matrix.[42] Moreover, above T_g, when materials became soft, reinforcement effect of the sc-PLA becomed prominent and hence strong enhancement of modulus appeared.[43]

Figure 7(b) delineated the variations of tanδ as a function of temperature. T_g was obtained from the tanδ peak temperature.

Table II. Storage Modulus Values of Neat PCL and Its Composites at Different Temperatures

Samples	Storage modulus at −75°C (MPa)	Storage modulus at 0°C (MPa)
Neat PCL	3331	535
PCL5	3493	627
PCL10	3558	725
PCL20	3441	885
PCL30	3607	1104

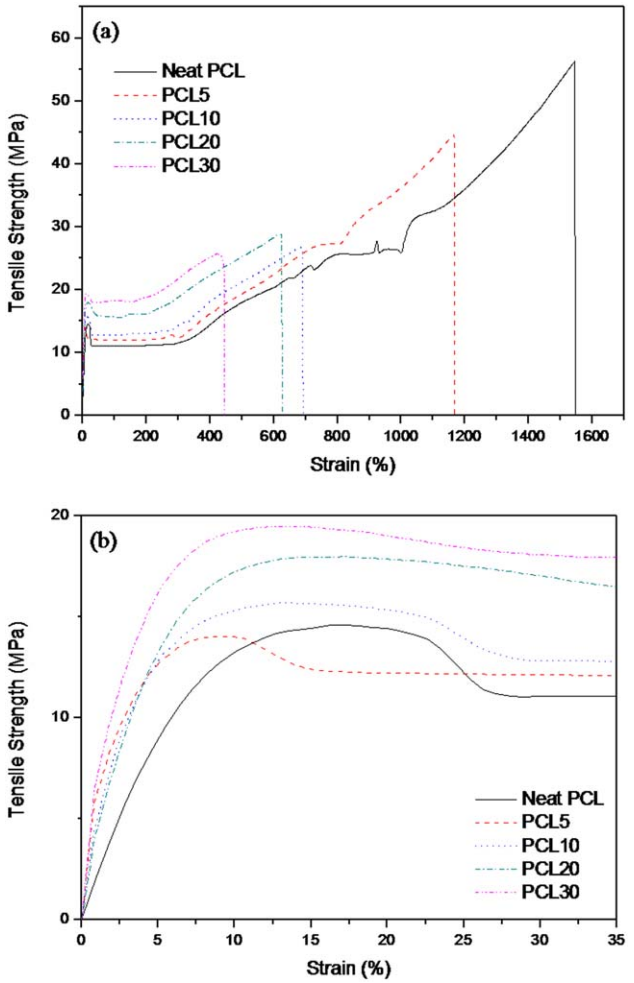

Figure 8. (a) Tensile stress–strain curves of neat PCL and its composites with different compositions: (b) gives details of tensile stress at low strain of (a). [Color figure can be viewed in the online issue, which is available at wileyonlinelibrary.com.]

Table III. Tensile Properties of Neat PCL and Its Composites

Samples	Modulus (MPa)	Tensile strength (MPa)	Elongation at break (%)	Yield Strength (MPa)
Neat PCL	358 ± 18	56.1 ± 1.3	1533 ± 67	14.27 ± 0.31
PCL5	564 ± 51	45.1 ± 5.6	1233 ± 167	14.16 ± 0.14
PCL10	634 ± 13	32.7 ± 6	895 ± 205	15.35 ± 0.35
PCL20	696 ± 41	29.6 ± 0.8	635 ± 5	18.15 ± 0.17
PCL30	776 ± 13	27.2 ± 1.5	490 ± 40	19.57 ± 0.10

As shown in Figure 7(b), the T_g values of PCL decreased slightly compared with the neat PCL at low sc-PLA loading. However, with an increase in sc-PLA loadings, the T_g values were hardly changed, which has been ascribed to the unrestricted segmental motions at the interface between PCL and sc-PLA.

Static Mechanical Properties

The effects of blending with sc-PLA on the static mechanical properties of PCL were investigated by tensile tests. Typical stress–strain curves of neat PCL and its composites were shown in Figure 8, and the detailed data of the mechanical properties were summarized and listed in Table III. The neat PCL showed higher stress and strain at break, almost reached to 56.1 MPa and 1533%, respectively, but had lower tensile yield strength and modulus. With the addition of sc-PLA, the tensile yield strength and modulus increased. The tensile yield strength of neat PCL was around 14.27 MPa, and the modulus was around 358 MPa. With increasing sc-PLA content, the tensile yield strength and modulus increased significantly, and for the composite with 30 wt % sc-PLA, the tensile yield strength and modulus increased to 19.57 and 776 MPa, respectively, which increased by 31.1 and 116.8%, respectively. This indicated that PCL was obviously reinforced by the sc-PLA, which was in accordance with the DMA results. The results of mechanical properties of both neat PCL and its composites with sc-PLA also might be influenced by the degree of crystallinity values of PCL. Therefore, Table IV shows the degree of crystallinity of PCL component in the composites prepared via the compression-molded process. From Table IV, it was clear that T_m and the degree of crystallinity of PCL component slightly decreased after the addition of sc-PLA, indicating that the reinforcement effect of the composites was mainly derived from sc-PLA. The reinforcement effect of the sc-PLA might be explained by the fact that the sc-PLA acts as carriers of load and stress was transferred from the matrix along the sc-PLA giving rise to effective and uniform stress distribution, resulting in an increase in tensile yield strength and modulus of the PCL/sc-PLA composites.[44] However, the elongation and strength at break gradually decreased with increasing the sc-PLA content. It should be noted that there was a strain-hardening phenomenon after the yield of the neat PCL due to the orientation of PCL molecules during tensile tests and the strain-hardening ability was very strong, which leaded to a high strength at break. As for the PCL/sc-PLA composites, the strain-hardening capacity of the composites decreased gradually with the increase of the sc-PLA. It was because that the presence of sc-PLA in the composites acting as impurity hindered the mobility of the macromolecular chains and molecular orientation during tension thereby contributing to the overall reduction in the elongation at break and the strain-hardening ability.[45] In addition, because of the discontinuous reinforcement of the sc-PLA and the immiscible of the PCL and sc-PLA, the stress and strain at break lowed rapidly. Combined with the results of rheology and mechanical characterization, the composite with 10 wt % sc-PLA showed optimal rheology and mechanical property; its tensile yield strength, Young's modulus, and elongation at break were 15.35 MPa, 634 MPa, and 895%, respectively.

Table IV. Thermal and Crystalline Properties of PCL in the Composites Obtained from the First Heating Traces at a Rate of 10°C/min

Samples	T_m (°C)	ΔH_m[a] (J/g)	$\chi_{c,PCL}$ (%)
Neat PCL	61.0	73.0	51.4
PCL5	60.4	66.5	46.8
PCL10	60.1	65.6	46.2
PCL20	60.0	71.5	50.4
PCL30	60.0	61.7	43.5

[a] ΔH_m are corrected for the content of PCL in the composites.

CONCLUSIONS

Environment-friendly composites of PCL/sc-PLA with different sc-PLA loadings were prepared by solution casting to investigate the effects of sc-PLA loadings on the crystallization, viscoelasticity, and mechanical properties of the PCL/sc-PLA composites. The following conclusions were obtained:

1. The sc-PLA components could not be distinguished from PCL matrix in ESEM photographs. This might be due to the good compatibility between PCL and sc-PLA.
2. DSC and WAXD demonstrated the formation of the stereocomplex in the blends and the addition of sc-PLA did not alter the crystal structure of PCL.
3. Rheological measurements indicated that the PCL/sc-PLA composites exhibited evident solid-like response in the low frequency region and the relaxation time increased considerably as the sc-PLA loadings reached up to 20 wt %. Moreover, at this loading level, the percolated sc-PLA network

structures formed and the long-range motion of PCL chains was highly restrained.
4. DMA showed that E' of PCL in the composites increased 106% as compared with that of the neat PCL at 0°C. The T_g values were hardly changed, which has been ascribed to the unrestricted segmental motions at the interface between PCL and sc-PLA.
5. Static mechanical properties showed that with the increase in sc-PLA content, the tensile yield strength, and modulus of the PCL composites increased significantly, indicating that significant reinforcement effect was achieved by adding sc-PLA. However, the elongation and strength at break decreased with the increase of the sc-PLA due to the hindered mobility and orientation of the PCL macromolecular chains during tension.

ACKNOWLEDGMENTS

This work is supported by the National Science Foundation of China (51021003, 50703042). Part of this work is supported by Jilin Province Science and Technology Agency (20116025) and Jilin Jianzhu University (862107).

REFERENCES

1. Antolín-Cerón, V. H.; Gómez-Salazar, S.; Rabelero, M.; Soto, V.; Luna-Bárcenas, G.; Katime, I.; Nuño-Donlucas, S. M. *Polym. Compos.* **2012**, *33*, 562.
2. Avella, M.; Errico, M. E.; Laurienzo, P.; Martuscelli, E.; Raimo, M.; Rimedio, R. *Polymer* **2000**, *41*, 3875.
3. Tsuji, H.; Yamada, T. *J. Appl. Polym. Sci.* **2003**, *87*, 412.
4. Ikada, Y.; Tsuji, H. *Macromol. Rapid Commun.* **2000**, *21*, 117.
5. Wang, L.; Ma, W.; Gross, R. A.; McCarthy, S. P. *Polym. Degrad. Stab.* **1998**, *59*, 161.
6. Wischke, C.; Löbler, M.; Neffe, A. T.; Hanh, B. D.; Zierke, M.; Sternberg, K.; Schmitz, K. P.; Guthoff, R.; Lendlein, A. *Macromol. Symp.* **2001**, *309/310*, 59.
7. Xing, Z. M.; Yang, G. S. *J. Appl. Polym. Sci.* **2010**, *115*, 2747.
8. Li, Y.; Han, C. Y.; Bian, J. J.; Zhang, X.; Han, L. J.; Dong, L. S. *Polym. Compos.* **2013**, *34*, 131.
9. Li, Y.; Han, C. Y.; Bian, J. J.; Zhang, X.; Han, L. *J. Polym. Compos.* **2013**, *34*, 1620.
10. Lim, J.; Chong, M. S. K.; Teo, E. Y.; Chen, G. Q.; Chan, J. K. Y.; Teoh, S. H. *J. Biomed. Mater. Res. B.* **2013**, *101B*, 752.
11. Liang, Y. G.; Yang, F.; Qiu, Z. B. *J. Appl. Polym. Sci.* **2012**, *124*, 4409.
12. Tsuji, H.; Takai, H.; Saha, S. K. *Polymer* **2006**, *47*, 3826.
13. Li, S. M.; Liu, L. J.; Garreau, H.; Vert, M. *Biomacromolecules* **2003**, *4*, 372.
14. Mallek, H.; Jegat, C.; Mignard, N.; Abid, M.; Abid, S.; Taha, M. *J. Appl. Polym. Sci.* **2013**, *129*, 954.
15. Wu, D. F.; Zhang, Y. S.; Zhang, M.; Yu, W. *Biomacromolecules* **2009**, *10*, 417.
16. Chen B. Q.; Evans, J. R. G. *Macromolecules* **2006**, *39*, 747.
17. Messersmith, P. B.; Giannelis, E. P. *J. Polym. Sci. Part A: Polym Chem.* **1995**, *33*, 1047.
18. Namazi, H.; Mosadegh, M. *J. Polym. Environ.* **2011**, *19*, 980.
19. Xu, Z. H.; Zhang, Y. Q.; Wang, Z. G.; Sun, N.; Li, H. *Appl. Mater. Interfaces* **2011**, *3*, 4858.
20. Li, Y.; Han, C. Y.; Bian, J. J.; Han, L. J.; Dong, L. S.; Gao, G. *Polym Compos.* **2012**, *33*, 1719.
21. Avella, M.; Bondioli, F.; Cannillo, V.; Pace, E. D.; Errico, M. E.; Ferrari, A. M.; Focher, B.; Malinconicoa, M. *Compos. Sci. Technol.* **2006**, *66*, 886.
22. Dong, Q. L.; Li, Y.; Han, C. Y.; Zhang, X.; Xu, K.; Zhang, H. L.; Dong, L. S. *J. Appl. Polym. Sci.* **2013**, *130*, 3919.
23. Woo, E. M.; Chang, L. *Polymer* **2011**, *52*, 6080.
24. Zhang, X.; Li, Y.; Han, L. J.; Han, C. Y.; Xu, K.; Zhou, C.; Zhang, M. Y.; Dong, L. S. *Polym. Eng. Sci.* **2013**, *53*, 2498.
25. Pan, H.; Qiu, Z. B. *Macromolecules* **2010**, *43*, 1499.
26. Chang, L.; Woo, E. M. *Polym. Eng. Sci.* **2012**, *52*, 1413.
27. Chang, L.; Woo, E. M. *Polymer* **2011**, *52*, 68.
28. Tsuji, H. *Macromol. Biosci.* **2005**, *5*, 569.
29. Ikada, Y.; Jamshidi, K.; Tsuji, H.; Hyon, S. *Macromolecules* **1987**, *20*, 906.
30. Li, Y.; Han, C.Y. *Ind. Eng. Chem. Res.* **2012**, *51*, 15927.
31. Lu, L. L.; Wu, D. F.; Zhang, M.; Zhou, W. D. *Ind. Eng. Chem. Res.* **2012**, *51*, 3682.
32. Martello, M. T.; Hillmyer, M. A. *Macromolecules* **2011**, *44*, 8537.
33. Cohn, D.; Salomon, A. H. *Biomaterials* **2005**, *26*, 2297.
34. Akos, N. I.; Wahit, M. U.; Mohamed, R.; Yussuf, A. A. *Polym. Compos.* **2013**, *34*, 763.
35. Tsuji, H.; Ikada, Y. *J. Appl. Polym. Sci.* **1996**, *60*, 2367.
36. Crescenzi, V.; Manzini, G.; Calzolari, G.; Borri, C. *Eur. Polym. J.* **1972**, *8*, 449.
37. Han, C. Y.; Ran, X. H.; Su, X.; Zhang, K. Y.; Liu, N. A.; Dong, L. S. *Polym. Int.* **2007**, *56*, 593.
38. Pan, H.; Yu, J.; Qiu, Z. B. *Polym. Eng. Sci.* **2011**, *51*, 2159.
39. Han, C. D.; Kim, J. K. *Polymer* **1993**, *34*, 2533.
40. Nie, K.; Zheng, S. X.; Lu, F.; Zhu, Q. R. *J. Polym. Sci. Part B: Polym. Phys.* **2005**, *43*, 2594.
41. Cole, K. S.; Cole, R. H. *J. Chem. Phys.* **1941**, *9*, 341.
42. Hudaa, M. S.; Drzala, L. T.; Mohanty, A. K.; Misra, M. *Compos. Sci. Technol.* **2006**, *66*, 1813.
43. Ray, S. S.; Yamada, K.; Okamoto, M.; Ueda, K. *Polymer* **2003**, *44*, 857.
44. Zhang, Y. H.; Yu, C. X.; Chu, P. K.; Lv, F. Z.; Zhang, C.; Ji, J. H.; Zhang, R.; Wang, H. L. *Mater. Chem. Phys.* **2012**, *133*, 845.
45. Tsuji, H.; Ishizaka, T. *Int. J. Biol. Macromol.* **2001**, *29*, 83.